Cellular & Molecular Immunology www.nature.com/cmi

ARTICLE

The metabolic regulator Lamtor5 suppresses inflammatory signaling via regulating mTOR-mediated TLR4 degradation

Wei Zhang[1], Ningtong Zhuang[2], Xiaoyi Liu[1], Long He[1], Yan He[2], Paween Mahinthichaichan[3], Hang Zhang[2], Yanhua Kang[2], Yin Lu[4], Qinan Wu[5], Dakang Xu[2,6,7] and Liyun Shi[1,2]

Comprehensive immune responses are essential for eliminating pathogens but must be tightly controlled to avoid sustained immune activation and potential tissue damage. The engagement of TLR4, a canonical pattern recognition receptor, has been proposed to trigger inflammatory responses with different magnitudes and durations depending on TLR4 cellular compartmentalization. In the present study, we identify an unexpected role of Lamtor5, a newly identified component of the amino acid-sensing machinery, in modulating TLR4 signaling and controlling inflammation. Specifically, Lamtor5 associated with TLR4 via their LZ/TIR domains and facilitated their colocalization at autolysosomes, preventing lysosomal tethering and the activation of mTORC1 upon LPS stimulation and thereby derepressing TFEB to promote autophagic degradation of TLR4. The loss of Lamtor5 was unable to trigger the TFEB-driven autolysosomal pathway and delay degradation of TLR4, leading to sustained inflammation and hence increased mortality among Lamtor5 haploinsufficient mice during endotoxic shock. Intriguingly, nutrient deprivation, particularly leucine deprivation, blunted inflammatory signaling and conferred protection to endotoxic mice. This effect, however, was largely abrogated upon Lamtor5 deletion. We thus propose a homeostatic function of Lamtor5 that couples pathogenic insults and nutrient availability to optimize the inflammatory response; this function may have implications for TLR4-associated inflammatory and metabolic disorders.

Keywords: TLR4; Lamtor5; mTORC1; TFEB; Autolysosome

Cellular & Molecular Immunology (2020) 17:1063–1076; https://doi.org/10.1038/s41423-019-0281-6

INTRODUCTION

Mammalian Toll-like receptors (TLRs) are evolutionally conserved sensors of pathogen-associated molecular patterns that play a central role in host defense against infection and injury.[1,2] Appropriately controlled immune responses are essential for eliminating injurious agents and maintaining homeostasis, whereas excessive immune and inflammatory responses cause tissue damage.[3] Dysregulated TLRs and downstream signaling molecules are therefore major players in various disorders such as infections, inflammatory, and metabolic diseases and cancers. Among known TLRs, TLR4 is distinguished by its ability to recognize a variety of exogenous and endogenous agents and activate different signaling pathways depending on its cellular localization.[4] Upon ligation, TLR4 dimerizes and associates with the TIR domain-containing adaptors TIRAP and myeloid differentiation primary response88 (MyD88), initiating signaling at the plasma membrane to drive NF-κB-mediated production of proinflammatory cytokines. Concurrently, engaged TLR4 is transferred to endosomes, where it activates Toll/IL-1R domain-containing adaptor and inducing IFN (TRIF) and the interferon factor (IRF)3-dependent production of interferon (IFN)-β.[5–7] Alternatively, TLR4 is transported to the degradative lysosome, where it contributes to signaling termination, or sorted to the recycling endosome for return to the cellular surface.[8–11] Thus, the intracellular trafficking and subcellular compartmentalization of TLR4 constitute a key mechanism that dictates the direction and amplitude of inflammatory signaling.[12,13] In particular, cellular degradation systems, such as lysosome- and proteasome-mediated catabolic processes, play a pivotal role in controlling TLR4 destiny and immune homeostasis.

Autophagy is a conserved cellular catabolic process that can involve the digestion of intracellular protein aggregates, damaged organelles, and invasive microorganisms.[14] Autophagy is initiated by the engulfment of large cytoplasmic portions and the formation of double membrane autophagosomes that subsequently fuse with endosomes and lysosomes, leading to the degradation and clearance of the sequestered contents.[15] The disruption of autophagy, which has been described as a

[1]Department of Immunology and Medical Microbiology, Nanjing University of Chinese Medicine, 210046 Nanjing, China; [2]Key Lab of Inflammation and Immunoregulation, Hangzhou Normal University School of Medicine, Hangzhou, 310036 Zhejiang, China; [3]University of Maryland, College Park, MD 20742, USA; [4]Jiangsu Key Laboratory for Pharmacology and Safety Evaluation of Chinese Materia Medica, Nanjing University of Chinese Medicine, 210046 Nanjing, China; [5]The College of Pharmacology, Nanjing University of Chinese Medicine, 210023 Nanjing, China; [6]Faculty of Medical Laboratory Science, Ruijin Hospital, School of Medicine, Shanghai Jiao Tong University, 227 Chongqing Road South, 200025 Shanghai, China and [7]Hudson Institute of Medical Research, Department of Molecular and Translational Science, Monash University, Clayton, VIC 3800, Australia
Correspondence: Liyun Shi (shi_liyun@msn.com)
These authors contributed equally: Wei Zhang, Ningtong Zhuang

Received: 11 August 2019 Accepted: 13 August 2019
Published online: 29 August 2019

cytoprotective response to stressful conditions, is associated with a myriad of diseases including inflammatory disorders.[16,17] Loss of the autophagic components autophagy-related 16 like 1, Beclin1, and microtubule-associated protein 1A/1B light chain 3 (LC3) enhanced the macrophage response to LPS, a prototypical agonist of TLR4, and caused sustained inflammatory signaling.[18,19] TLR4 engagement has been demonstrated to trigger the formation of $LC3^+$ structures and activate the autophagosomal pathway, which in turn causes the eradication of inflammatory initiators such as invading pathogens and mitochondrial ROS and DNA release[20,21] or the degradation of key signaling molecules such as TRIF, NF-κB, and pellino E3 ubiquitin protein ligase family member 3 (Peli3).[22–24] Studies have shown the critical involvement of autophagy in TLR signaling, but the direct relevance of autophagy to TLR4 turnover has not been explored.

Late endosomal/lysosomal adaptor, mitogen-activated protein kinase (MAPK) and mTOR activator (Lamtor)5 is a highly conserved, ~18 kDa protein originally identified as a hepatitis type B x protein-interacting protein.[25] Lamtor5 associates with the oncogenic proteins c-FOS and c-Myc as well as Survivin and p53, promotes proliferation and exerts antiapoptotic effects in cancer cells.[26–28] A recent study identified Lamtor5 as an indispensable component of the Ragulator complex that interacts with small GTPase Ras-related GTP binding protein (RAG), contributing to lysosomal recruitment and the activation of mechanistic target of rapamycin complex 1 (mTORC1) in response to amino acids.[29,30] mTORC1 is a master growth regulator whose translocation to the lysosomal surface, the site of mTORC1 activation, is stimulated by amino acids and GTPase. As a result, the mTOR pathway couples amino acid availability to cell growth and autophagy.[31,32] In this process, Lamtor5, in combination with other Lamtor proteins, serves as a guanine exchange factor (GEF) for RAG GTPase to transduce nutrient-sensing signaling. GEFs, molecular switches that control the GTP-bound 'on' and GDP-bound 'off' statuses of GTPase, play a key role in integrating extracellular signals initiated from surface receptors to intracellular pathways. GEFs have been implicated in diverse cellular processes such as receptor recycling, synaptic vesicle endocytosis, and protein transport. Recent studies have indicated that the GEFs RAB guanine nucleotide exchange factor 1, Ras guanine nucleotide releasing protein 3, and DENN domain-containing B1 are critically involved in inflammatory and allergic processes,[33–35] implying the expanding roles of GEFs in immunological contexts.

In the present study, we reveal the unexpected key role of Lamtor5 in regulating TLR4 intracellular fate and immune homeostasis. Specifically, Lamtor5 directly interacts with internalized TLR4 and facilitates their colocalization at autolysosomes, preventing mTORC1 recruitment to lysosomes and facilitating nuclear translocation of transcription Factor EB (TFEB)[36], hence promoting the autophagic degradation of TLR4. Accordingly, the depletion of Lamtor5 delays TLR4 degradation and sustains inflammatory signaling, leading to increased susceptibility to endotoxic sepsis. In addition, Lamtor5 was shown to largely mediate the anti-inflammatory action of nutrient deprivation, particularly leucine depletion. We have thus identified a critical role for Lamtor5 in TLR4 biology and inflammatory regulation that provides a potential molecular link between immune and metabolic processes.

MATERIALS AND METHODS

Reagents and antibodies

LPS from *Escherichia coli* O111:B4, chloroquine (CQ) (C6628), *L*-leucine (L8912), and a Myeloperoxidase (MPO) Fluorometric Activity Assay Kit (MAK069) were purchased from Sigma (St. Louis, MO). Bafilomycin A1 (Baf-A1) (S1413), torin 1 (S2827), U0126 (S1102), SB203580 (S1076), LY2904002 (S1105), BAY11-7082 (S2913), SP600125 (S1460), and vinblastine (S4505) were obtained from Selleck Chemicals (Shanghai, China). Dynabeads™ Protein A for Immunoprecipitation (10002D) and DQ-BSA (D-12050) were purchased from Thermo Fisher Scientific (Waltham, MA). Enzyme-linked immunoassay kits for IL-6, IL-1β, and TNF-α were obtained from R&D Systems (Minneapolis, MN).

Antibodies (Abs) specific for total and phosphorylated forms of p38 (Thr180/Tyr182), ERK1/2 (Thr202/Tyr204), JNK (Thr183/Tyr185), p65 (Ser536), IKKα/β (Ser176), TAK1 (Thr187), AKT (Ser473), mTOR (Ser2448), p70 S6 Kinase (Thr421/Ser424), 4E-binding protein 1 (4E-BP1) (Thr37/46), ULK1 (Ser757), IRF3 (Ser396), and IκBα (Ser32) were obtained from Cell Signaling Technology (Beverly, MA). Abs against Lamtor5 (ab157480), TLR4 (ab22048 and ab13556), TFEB (ab2636), Rab7 (ab50533), p62 (ab56416), and EEA1 (ab2900) were obtained from Abcam. Abs against FLAG (#14793 and #8146), GFP (#2956 and #2955), LC3A/B (#4108), LC3B (#3868), lysosomal-associated membrane protein (LAMP1) (#3243), and β-actin (#4970) were obtained from Cell Signaling Technology (Beverly, MA). Horseradish peroxidase-conjugated secondary antibody was purchased from Santa Cruz Biotechnology (Santa Cruz, CA). Alexa Fluor-conjugated antibodies were purchased from Life Technologies (Carlsbad, CA).

Lamtor5-, TFEB-, Atg5-, and Rab7-targeted siRNAs and non-specific siRNA were synthesized from GenePharma (Shanghai, China). The pEGFP-LC3 (#24920) and ptfLC3 (#21074) plasmids were purchased from Addgene. The pRL-TK-Renilla-luciferase plasmid was obtained from Promega (Madison, WI). The full-length fragments of Lamtor5 (NM_026774.2) and TLR4 (NM_021297.3) were cloned and inserted into the pCMV-Tag 2B or pEGFP vectors, respectively, using standard molecular biology protocols. Expression plasmids encoding Lamtor5, Lamtor5 mutants (ΔLZ), and truncated TLR4 proteins were constructed by GeneChem (Shanghai, China).

Generation of Lamtor5 knockout mice

The CRISPR/Cas9 technique was used to edit Lamtor5 in mice by CasGene Biotech (Beijing, China). Small guide RNAs (sgRNAs) targeting exons 1–3 of Lamtor5 were designed and constructed. sgRNA-Cas9 coexpression plasmids were injected into mouse zygotes, which were then transferred into pseudopregnant mice. Neonatal mutant mice were identified by genotyping and sequencing.[37]

Cell culture and transfection

RAW264.7 cells (ATCC® TIB-71™) and 293T cells (ATCC® CRL-3216™) were cultured in DMEM-containing 10% fetal bovine serum (FBS). THP-1 cells (ATCC® TIB-202™) were cultured in RPMI-1640 medium supplemented with 10% FBS in a humidified incubator at 37 °C with 5% CO_2. To generate peritoneal macrophages, 8-week-old mice were injected i.p. with 3% thioglycolate broth. After 72 h, peritoneal cells were harvested, and macrophages were enriched by quick adherence.

For cell transfection, RAW264.7 or 293T cells were transiently transfected with plasmids using X-tremeGENE Transfection Reagent (Roche) or siRNAs using siPORT™ Transfection Agent (Thermo Fisher Scientific) according to the manufacturer's instructions. To establish stable Lamtor5-expressing or Lamtor5-silenced cell lines, the transfected cells were subjected to selection with G418 (600 μg/ml) for 3–4 weeks.

RNA isolation, reverse transcription PCR, and quantitative PCR

Total cellular RNA was isolated using TRIzol reagent (Invitrogen). SYBR Green PCR Master Mix (TOYOBO) was used to detect mRNA levels. mRNA levels of the tested genes were normalized to those of β-actin and determined by applying the ΔΔCt method. The following primer sequences were used (forward and reverse):

IL-1β: 5′-CTCGTGCTGTCGGACCCAT and 5′-CAGGCTTGTGCTCTGCTTGTGA; *IL-6*: 5′-CCACTTCACAAGTCGGAGGC and 5′-TGCAAGTGCATCATCGTTGTTC; *TNF-α*: 5′-ATCCGCGACGTGGAACTGGC

and 5′-CCATGCCGTTGGCCAGGAGG; *IFN-β*: 5′-CAGTAATAGCTCTTC AAGTGG and 5′-AGACTATTGTTGTACGTCTCC; *TLR4*: 5′-AACCTGCTC TACCTACACCTG and CCGAGAGATTGAGGAATCGAAG; *β-actin*: 5′-CTCATGAAGATCCTGACCGAG and 5′- AGTCTAGAGCAACATAGCAC AG; and *Lamtor5*: 5′-CATCCATTGTTGGAGTCCTATGC and 5′-TGCT GGGCTAGAACAGATATGA.

Immunoblot analysis and coimmunoprecipitation assay

Cell lysates were prepared in a lysis buffer containing 150 mM NaCl, 50 mM Tris-HCl (pH 7.4), 1% NP-40 and protease inhibitor cocktail (Roche Diagnostics). Proteins were separated by SDS-PAGE and transferred to PVDF membranes followed by incubation with the appropriate primary antibodies. The membranes were then incubated with HRP-conjugated secondary antibody (Santa Cruz, CA). Signals were visualized with an ECL kit (Amersham Biosciences). Images were captured using a ChemiDoc™ XRS+ system (Bio-Rad, USA). Band detection was within the linear range.

For immunoprecipitation studies, cell lysates were incubated at 4 °C for 2 h with a capture antibody or control IgG, followed by overnight incubation with Dynabeads™ Protein A. The immunocomplexes were collected by centrifugation, washed with ice-cold PBST (PBS-0.02% Tween-20), and separated by SDS-PAGE. Proteins in the samples were detected by standard immunoblotting methods.

Luciferase reporter assay

To assess NF-κB-driven promoter activity, the pGL3-NF-κB, and pGL3-Basic (Promega) plasmids were transfected into RAW264.7 cells using X-tremeGENE DNA Transfection Reagent (Roche). The pRL-TK plasmid was used as an internal control. Twenty-four hours later, the cells were stimulated with or without LPS (100 ng/ml) for 1 h. Luciferase activities were determined with Dual-Glo reagent (E1960, Promega).[38]

Determination of cytokine and MPO Levels

The levels of TNF-α, IL-6, and IL-1β in the culture supernatants or bronchoalveolar lavage fluid (BALF) were measured by ELISA (R&D Systems). Lung MPO levels were determined using mouse MPO ELISA (Hycult Biotech) following the manufacturers' instructions.

Animal experiments

All of the animal experiments were performed in accordance with the National Institutes of Health Guide for the Care and Use of Laboratory Animals with the approval of the Animal Care and Use Committee of Nanjing University of Chinese Medicine. The CRISPR/Cas9 technique[37] was used to edit Lamtor5 in mice. Mice were housed in a temperature-controlled room with a 12-h-light/dark cycle and allowed food and water ad libitum. Six- to eight-week-old Lamtor5$^{+/-}$ or wild-type (WT) mice were instilled with PBS or LPS (1 mg/kg, i.t.) and killed 12 or 24 h after exposure. BALF and lung tissues were then collected for functional analysis. To induce endotoxic sepsis, mice were intraperitoneally injected with LPS (12 mg/kg), and their survival was monitored every 4 h. Alternatively, prior to endotoxin challenge, mice were fed a rodent diet (Research Diet, A10021B) or leucine-free diet (Research Diet, A05080202) for a week.[39]

Bronchoalveolar lavage and cell differentiation

Briefly, the trachea was exposed through a midline incision and cannulated with a sterile 22-gauge needle. BALF was obtained by flushing three times with 1 ml of 0.5 mM EDTA/PBS. The supernatants were stored at −80 °C until use. Total cell numbers in BALF were counted with a hemocytometer. Neutrophils and macrophages were assessed through immunostaining and flow cytometry.

Immunohistochemistry (IHC) staining

Five-micron-thick sections of murine lung tissue were deparaffinized, hydrated, and blocked in DPBS with 2% normal goat serum. The slides were then stained with anti-Lamtor5 (1:100) and biotin-conjugated secondary antibodies, followed by incubation with streptavidin-conjugated HRP. Sections were finally incubated with DAB reagent and counterstained with hematoxylin.

Flow cytometry and lysosome labeling

After blocking unspecific binding with mouse IgG, cells were incubated with 0.25 μg of PE-conjugated anti-mouse TLR4 antibody (eBioscience) for 1 h at room temperature. Appropriate isotype controls were used. After washing twice in flow cytometry buffer, cells were analyzed on a FACSCalibur flow cytometer (BD Biosciences).

To evaluate functional lysosomes, the LysoSensor Green probe, which fluoresces in an acidic environment (pH ≤ 5.2), was used. RAW264.7 cells were loaded with 1 μM LysoSensor in prewarmed medium for 1 h at 37 °C, washed twice with PBS and immediately analyzed by flow cytometry. Data were analyzed with FlowJo (Tree Star).[40]

Immunofluorescence staining and DQ-BSA quench assay

Cells were grown on cover glasses, fixed with 4% paraformaldehyde, and[41] permeabilized with 0.2% Triton X-100 in PBS. After blocking with 1% BSA, cells were stained by incubation with primary antibodies (against TLR4, LAMP1, LC3, EEA1, mTOR, Lamtor5, or TFEB) for 16 h at 4 °C. After washing, samples were incubated with Alexa Fluor 568-conjugated anti-rabbit antibody and/or Alexa Fluor 488-conjugated anti-mouse antibody. Cell nuclei were visualized with DAPI (Sigma). Slides were mounted with SlowFade Gold anti-fade reagent (Invitrogen) and detected under a LSM710 laser scanning confocal microscope (Carl Zeiss). For the DQ-BSA quench assay, cells were treated with 0.3 mg/ml DQ Green BSA (molecular probe) at 37 °C for 2 h. Green fluorescence was detected by a Zeiss LSM 5 LIVE.

Electron microscopy

Cells were first fixed with 2.5% glutaraldehyde in PBS (0.1 M, pH 7.0) for 4 h, washed, and postfixed with 1% OsO_4 for 2 h. The specimen was dehydrated with a graded ethanol series for 20 min at each step, transferred to absolute acetone for 20 min, placed in a mixture of absolute acetone and resin overnight, and embedded in resin at 70 °C for more than 9 h. The specimen was then sectioned with a LEICA EM UC7 ultratome and stained with uranyl acetate and alkaline lead citrate for 5–10 min. Electron micrographs were taken on a JEOL Model JEM-1230 transmission electron microscopy (TEM).

The structural modeling and molecular dynamics (MD) simulation

The Lamtor5 dimer was modeled using the 1.5-Å resolution crystal structure deposited as PDB entry 3MSH. A disulfide bond was modeled between the two Cys66 residues located at the dimer interface and adjacent to each other. Because the structure of the TIR domain of TLR4 (residues 672–818) was not available in the PDB, a refined homology model was obtained using the I-TASSER webserver.[42] Using the first of five predicted models, the TIR-TLR4 dimer was modeled using the matrix operator provided for the TIR domain of TLR2 (PDB entry 1FYW), the sequence of which is most similar to that of TIR-TLR4.[43] A disulfide bond was modeled between the two Cys76 residues of TIR-TLR4, which are located at the dimer interface. The ClusPro webserver, which is widely accepted as a reliable docking program by CAPRI (critical assessment of predicted interactions), was used for protein–protein docking.

Lamtor5 dimer, TIR-TLR4 dimer, and Lamtor5-TLR4 complex simulations were performed using NAMD2[44] with a time step of 2 fs and the CHARMM36 force field. These simulations were all performed under the Generalized Born/Solvent-Accessible Surface Area (GB/SA) implicit solvent model implemented in NAMD[45] with both hydrophilic and hydrophobic effects taken into account. The solvent (ions and water molecules) was represented as a continuous medium with a solvent dielectric constant of 78.5

instead of individual explicit molecules. The born radius cutoff was set to 12 Å. All bonds involving hydrogen atoms were kept rigid using the SHAKE algorithm. The cutoff for van der Waals interactions was set to 14 Å with the switching distance set to 13 Å. The temperature was maintained at 310 K by Langevin dynamics with a damping coefficient of 5 ps^{-1}.

Statistical analysis

All experiments were performed at least three times. The results are expressed as the mean ± SD. Differences between two groups were established by Student's *t*-test. Multiple group comparisons were performed by one-way ANOVA followed by Bonferroni post hoc *t* test. $P < 0.05$ indicated statistical significance.

RESULTS

Lamtor5 is induced by TLR4 engagement and amino acid deprivation

To explore the potential role of Lamtor5 in innate immune responses, we first examined its expression in macrophages in response to an array of TLR ligands. Strikingly, Lamtor5 expression was induced by LPS, Pam3CSK4, poly I:C, CpG (Supplementary Fig. S1a–d) and the pathogenic agents *Staphylococcal aureus* (*S. aureus*) and vesicular stomatitis virus (Supplementary Fig. S1e, f). These findings indicated the involvement of Lamtor5 in PRR-mediated immune responses, and our attention was focused on TLR4 signaling given its central importance in immune and inflammatory responses. We further confirmed that LPS stimulation induced Lamtor5 in murine RAW264.7 macrophages and primary macrophages in a time- and dose-dependent manner (Fig. 1a–d). A similar increase in Lamtor5 levels was observed in human monocytic THP-1 cells and peripheral blood mononuclear cells (Fig. 1e–g). Moreover, the in vivo induction of Lamtor5 was demonstrated in murine lungs intratracheally challenged with endotoxin (Fig. 1h).

To understand the mechanism underlying TLR4-driven Lamtor5 expression, we applied specific inhibitors of phosphoinositide 3-kinase, MAPK, NF-κB, and mTOR signaling pathways, the key pathways downstream of TLR4. Lamtor5 expression was impaired by treatment with the NF-κB inhibitor BMS345541 and the ERK inhibitor U0126, although the effect of U0126 was less pronounced (Fig. 1i). Since Lamtor5 is a component of the amino acid-sensing machinery, we then assessed the impact of nutrient status on Lamtor5 expression. Unexpectedly, the deprivation of serum or leucine, an essential amino acid (EAA), profoundly increased Lamtor5 levels, whereas the addition of leucine reduced Lamtor5 expression (Fig. 1j, k). Taken together, our data indicate that Lamtor5 is induced in macrophages in response to cellular stresses such as pathogenic insult or nutrient insufficiency.

Lamtor5 suppresses inflammatory responses and alleviates endotoxic sepsis

To investigate the function of Lamtor5 in TLR4-induced immune and inflammatory responses, we generated Lamtor5-expressing and Lamtor5-silenced macrophage cell lines (Supplementary Fig. S2a, b). Remarkably, the enforced expression of Lamtor5 reduced the expression of the proinflammatory cytokines interleukin (IL)-6, IL-1β, and tumor necrosis factor (TNF)-α in response to LPS stimulation, whereas knockdown of Lamtor5 increased their expression (Fig. 2a–d). A similar increase in proinflammatory cytokine expression was induced in macrophages isolated from mice following the monoallelic depletion of Lamtor5, as homozygous gene knockout was embryonically lethal (Supplementary Fig. S3). This suppressive effect of Lamtor5 was also confirmed in human THP-1 cells following LPS challenge, implying its conserved role in inflammatory responses (Fig. 2e).

To further understand the in vivo relevance of this finding, we exploited a murine model of acute lung inflammation and injury induced by endotoxins. Compared with their control littermates, Lamtor5 haploinsufficient mice displayed more severe airway inflammation and tissue damage, as evidenced by increased inflammatory cell infiltration, proinflammatory cytokine production, protein leakage, and lung MPO activity (Fig. 2f–j). Furthermore, $Lamtor5^{+/-}$ mice exhibited elevated mortality compared with WT controls when challenged with lethal doses of endotoxin (Fig. 2k). Taken together, our data indicated that Lamtor5 plays a key role in restraining TLR4-mediated inflammatory signaling and maintaining immune homeostasis.

Lamtor5 restrains TLR4-induced inflammatory signaling

To gain mechanistic understanding of the Lamtor5-mediated regulation of inflammatory responses, we next analyzed the key signaling pathways downstream of TLR4. As revealed in Fig. 3a, b, enforced expression of Lamtor5 increased LPS-stimulated activation of IκB kinase (IKK), NF-κB inhibitor alpha (IκBα), and p65, the key signaling molecules required for NF-κB activation. In contrast, knockdown of Lamtor5 enhanced the phosphorylation of these molecules upon LPS stimulation. In addition, our data showed that NF-κB-driven promoter activity and the nuclear translocation of p65, the essential step for the activation of proinflammatory genes, were consistently repressed upon Lamtor5 overexpression but increased upon Lamtor5 silencing (Fig. 3c, d). The suppression of NF-κB activity by Lamtor5 was further confirmed in $Lamtor5^{+/-}$ macrophages (Fig. 3e). Activation of the MAPKs p38, ERK1/2, and JNK, however, was slightly affected by Lamtor5 (Fig. 3f, g).

In addition, Lamtor5 overexpression decreased, while Lamtor5 knockdown increased, the phosphorylation of TANK binding kinase 1 and IRF3, which was consistent with the modulated IFN-β expression upon LPS stimulation (Fig. 3h–k). Thus, our data indicated that Lamtor5 exerts an inhibitory effect on both NF-κB- and IRF3-dependent signaling upon the engagement of TLR4.

Lamtor5 promotes TLR4 degradation through the autophagic pathway

Given the comprehensive inhibition of TLR4 signaling by Lamtor5 observed as described above, we hypothesized that Lamtor5 affects key upstream signaling events and, in particular, the dynamic expression of TLR4. Indeed, our data demonstrated that enforced expression of Lamtor5 reduced, while the knockdown of Lamtor5 increased, TLR4 levels upon TLR4 engagement (Fig. 4a). $Lamtor5^{+/-}$ macrophages consistently displayed increased TLR4 levels (Fig. 4b). Notably, despite the prominent suppression of the TLR4 protein induced by Lamtor5, the TLR4 mRNA level was only mildly affected (Supplementary Fig. S4a, b). Furthermore, by fluorescent cytometry, we observed that surface TLR4 levels were reduced upon Lamtor5 overexpression but increased upon Lamtor5 deletion (Fig. 4c). Taken together, these data implied that Lamtor5 exerts a regulatory effect on TLR4 turnover upon TLR4 ligation. Since TLR4 is internalized upon engagement and subjected to different intracellular fates, we then evaluated the impact of Lamtor5 on TLR4 endocytosis by staining with EEA1, an endocytic marker. TLR4 localization at the endosome was not affected by Lamtor5 (Supplementary Fig. S4c). However, using the self-quenched fluorophore DQ-BSA[41], we showed that BSA hydrolysis was enhanced in Lamtor5-expressing cells but decreased in Lamtor5-silenced cells (Fig. 4d), indicating that Lamtor5 affects cellular degradation.

Given that autophagy is a major cellular catabolic process essential for the degradation of cellular components and proteins, we then assessed the potential role of the autophagic pathway in Lamtor5-mediated TLR4 regulation. Critically, Lamtor5 expression promoted, while Lamtor5 silencing impeded, the conversion of LC3-I to LC3-II and the stability of p62, which are key events representative of the autophagic pathway (Fig. 4e). In addition, the amplitude of the fluorescence at LC3 puncta was increased upon Lamtor5 overexpression but decreased by Lamtor5 deletion in LPS-stimulated macrophages

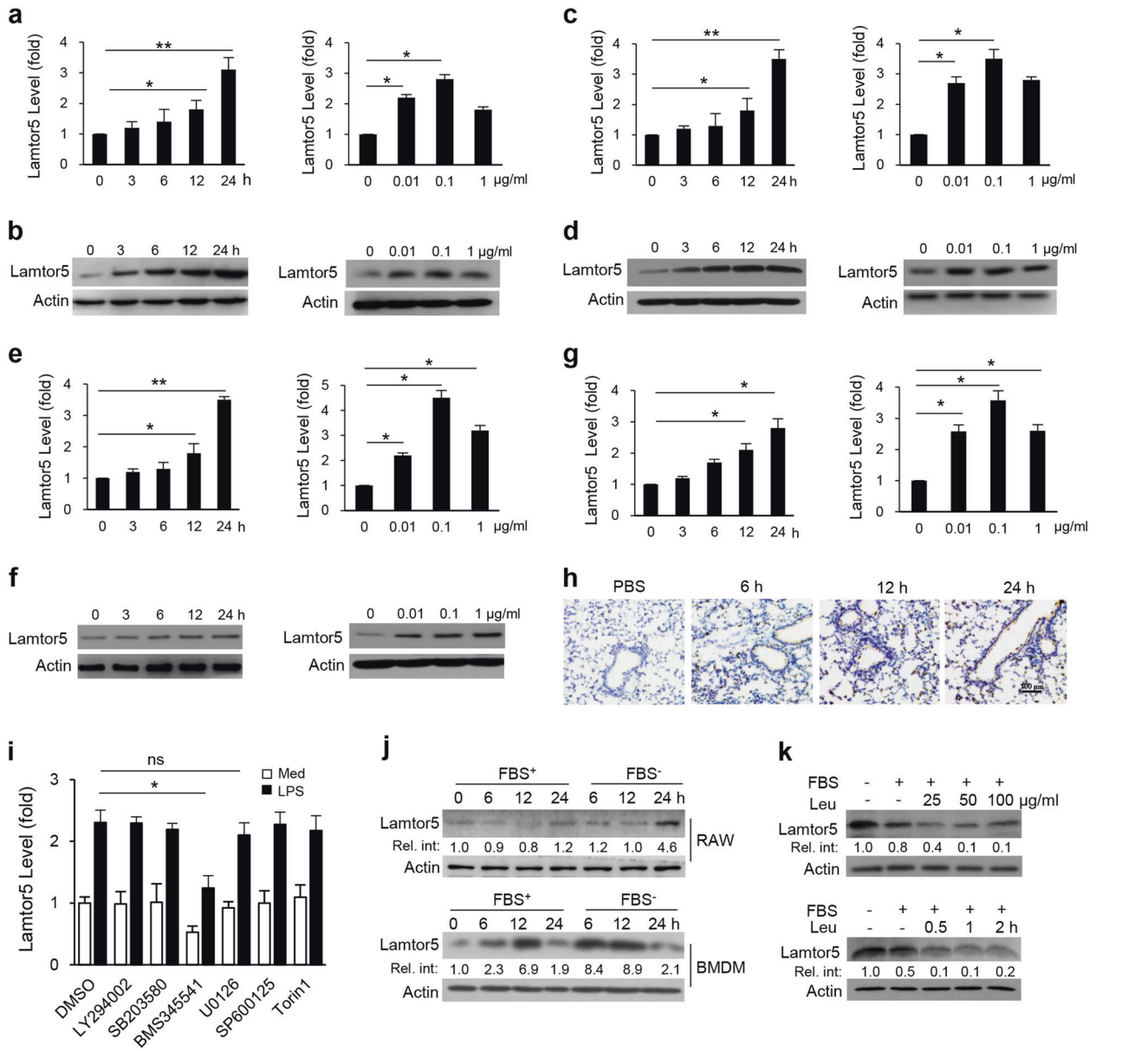

Fig. 1 Expression of Lamtor5 upon LPS stimulation and nutrient deprivation. Time- and dose-dependent expression of Lamtor5 following LPS stimulation in RAW264.7 cells (**a**, **b**), murine peritoneal macrophages (**c**, **d**), THP-1 cells (**e**, **f**), or human PBMCs (**g**). LPS (100 μg/ml) was used in the time course experiments, and a 12-h time point was used in experiments to assess the LPS dose. **h** Immunostaining of Lamtor5 in the lung tissues of mice intratracheally injected with PBS (24 h) or LPS (1 mg/kg) for the indicated time periods. **i** Expression of Lamtor5 in RAW264.7 cells pretreated with DMSO, LY294002 (10 μM), BMS345541 (10 μM), SB203580 (10 μM), U0126 (10 μM), SP600125 (20 μM), or torin 1 (250 nM) followed by LPS (100 ng/ml) stimulation for 6 h. **j** Lamtor5 expression in RAW264.7 cells or BMDMs cultured in the presence or absence of *fetal bovine serum* (FBS) for the indicated time periods. **k** Lamtor5 expression in RAW264.7 cells cultured in medium with or without leucine (Leu) and/or FBS. All the results are from three independent experiments and presented as the mean ± SD. **P* < 0.05, ***P* < 0.01 by Student's *t*-test

(Fig. 4f). We also confirmed that autophagic flux was induced in Lamtor5-expressing macrophages, as detected upon treatment with Baf-A1, a putative autophagy inhibitor (Fig. 4g). To corroborate the potential role of Lamtor5 in autophagy, we then analyzed its effect on the activity of mTOR, a critical regulator of autophagy induction. The activation of mTORC1, along with its downstream signaling molecules ribosomal protein S6 kinases, eukaryotic translation initiation factor 4E-BP1, and unc-51 like kinase (ULK)1, was repressed upon Lamtor5 overexpression but increased upon Lamtor5 deletion (Fig. 4h, i). Therefore, our data demonstrated that Lamtor5 contributes to the mTOR-dependent autophagic pathway in response to LPS stimulation.

Next, we determined whether inhibition of the Lamtor5-mediated autophagic pathway affects TLR4-driven signaling. To this end, Baf-A1 was used to block the autophagic process, which restored the TLR4 level and NF-κB activity (Fig. 4j) and led to the subsequent elevation of LPS-induced IL-6 and TNF-α in Lamtor5-expressing macrophages (Supplementary Fig. S5). In contrast, the application of torin 1, a putative mTOR inhibitor, downregulated TLR4 levels and p65 activity in Lamtor5-deficient macrophages following LPS stimulation (Fig. 4k). Consistent with this finding, the knockdown of autophagy protein (Atg)5, a key factor required for autophagosome elongation, largely abolished the Lamtor5-mediated suppression of TLR4 (Fig. 4l). Collectively, our data indicated that

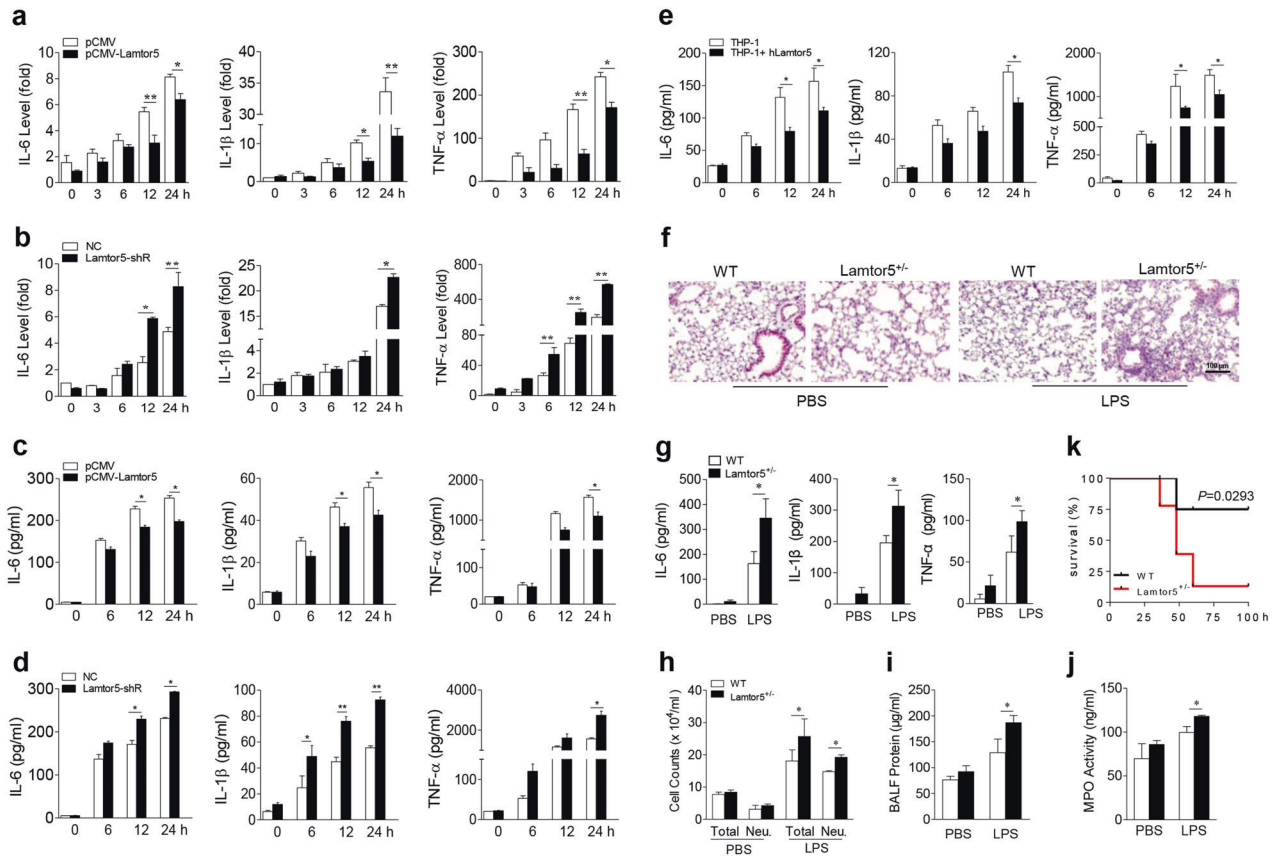

Fig. 2 Lamtor5 inhibits the LPS-induced inflammatory response in vitro and in vivo. Expression of IL-6, IL-1β, and TNF-α in control, Lamtor5-expressing, and Lamtor5-silenced RAW264.7 cells following LPS (100 ng/ml) stimulation at either the mRNA (**a**, **b**) or protein level (**c**, **d**). **e** Levels of IL-6, IL-1β, and TNF-α in control or Lamtor5-expressing THP-1 cells stimulated with LPS (100 ng/ml) for the indicated time periods. **f**–**j** WT and Lamtor5$^{+/-}$ mice ($n = 5$) were intratracheally instilled with LPS (1 mg/kg) and killed 12 h later. Representative H&E staining of lung sections (**f**); BALF cytokine levels (**g**), cell counts (**h**) and protein leakage (**i**); and lung MPO activity (**j**). **k** WT and Lamtor5$^{+/-}$ mice ($n = 10$–12) were challenged with LPS (12 mg/kg, i.p.), and their survival was analyzed by the Kaplan–Meier method. All the data are from three independent experiments (**a**–**e**) and expressed as the means ± SDs. *$P < 0.05$, **$P < 0.01$ by Student's *t*-test

Lamtor5 plays a pivotal role in promoting the mTOR-dependent autophagic pathway and hence reduces TLR4 levels and subsequent signaling.

Lamtor5 directly binds and recruits TLR4 to autophagosomes through the TIR/LZ interaction

During the induction of autophagy, substrate proteins or targeting organelles are sequestered in double membrane autophagosomes that then fuse with lysosomes for digestion. To further understand the mode of action of Lamtor5 in the autophagic process, we next examined its localization at autolysosomal compartments. Importantly, Lamtor5 colocalized with the autophagosome marker LC3b and LAMP1 (Fig. 5a, b), suggesting Lamtor5 tethering at autophagic/lysosomal vacuoles upon LPS stimulation in particular. Furthermore, upon its ligation, TLR4 was internalized and transported to the autolysosomal compartments, as inferred from its colocalization with LC3b and LAMP1, particularly that upon Lamtor5 overexpression (Fig. 5c, d). Using immunofluorescence confocal microscopy and coimmunoprecipitation (co-IP), we further revealed that Lamtor5 is prominently associated with TLR4 during TLR4 engagement (Fig. 5e, f). Thus, we have demonstrated for the first time that internalized TLR4 is trafficked to and resides at the autolysosome through the recruitment of Lamtor5.

To further understand the interaction between Lamtor5 and TLR4, we generated a series of expression constructs containing truncated *TLR4* fragments or *lamtor5* fragments (Fig. 5g). Loss of the leucine zipper (LZ) domain significantly impaired the association of Lamtor5 with TLR4 (Fig. 5h–j). More specifically, when we substituted Leu48 with Leu55 (L → A), the key residue essential for the LZ structure,[46] the interaction between Lamtor5 and TLR4 was inhibited (Fig. 5k). We further confirmed that the Toll/IL-1 receptor homology (TIR) domain, rather than leucine-rich repeat (LRR) domain,[47] within TLR4 is indispensable for this association (Fig. 5l, m). Accordingly, mutation of the Lamtor5 LZ domain or deletion of the extracellular domain of TLR4 caused a profound reduction in the TIR/LZ interaction (Fig. 5n, o). In addition, MD simulation[42,47] provided a structural basis to support the ligation of Lamtor5 and TLR4 (Fig. 5p). Therefore, our data demonstrated that Lamtor5 directly associates with TLR4 and contributes to their colocalization at the LC3^{+}LAMP1^{+} autophagosome for subsequent TLR4 hydrolysis. In support of this conclusion, LZ-mutant Lamtor5 lost its ability to interact with TLR4 and hence failed to suppress TLR4 levels (Fig. 5q).

Lamtor5 enhances lysosomal biogenesis through modulating the mTOR/TFEB axis

Since Lamtor5 was shown to recruit and colocalize with TLR4 at the autolysosome, a site generally thought to be occupied by mTORC1 upon amino acid induction,[29–32] we thus wondered whether mTORC1 participates in the Lamtor5/TLR4 interaction. Indeed, our data demonstrated the docking of mTORC1 at the LAMP1^{+} lysosome following LPS stimulation; however, this

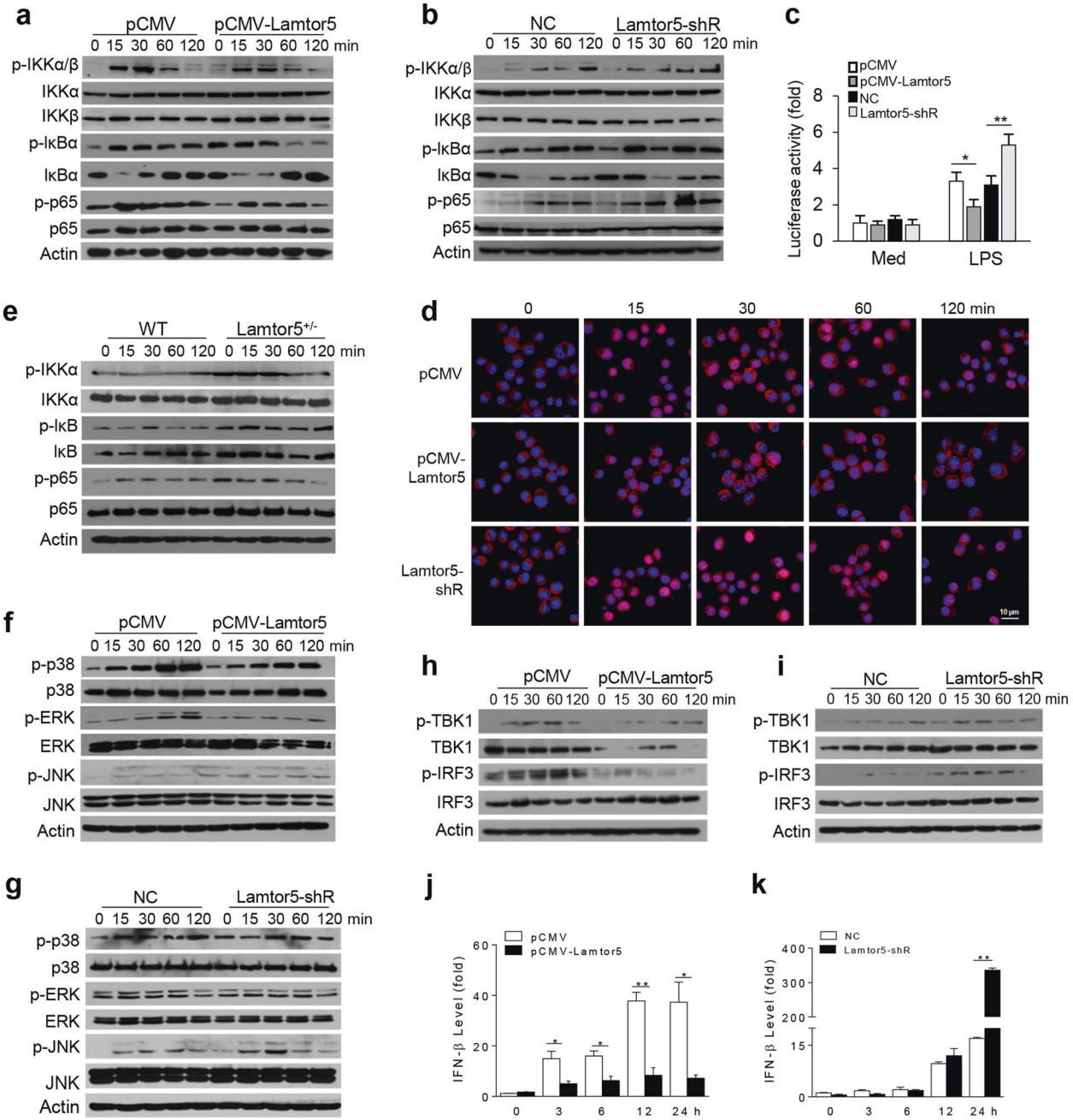

Fig. 3 Lamtor5 negatively regulates TLR4-driven signaling. **a, b** Immunoblotting of total and phosphorylated IKK, IκBα, and p65 in control, Lamtor5-expressing and Lamtor5-silenced RAW264.7 cells stimulated with LPS (100 ng/ml) for the indicated time periods. **c** Relative NF-κB promoter activity induced by LPS in control, Lamtor5-expressing and Lamtor5-silenced RAW264.7 cells. **d** Confocal microscopy analysis of p65 nuclear translocation upon stimulation with p65. p65 immunoreactivity is shown in red, and nuclei are stained with DAPI (blue). **e** Immunoblotting of total and phosphorylated IKK, IκBα, and p65 in WT and Lamtor5$^{+/-}$ cells stimulated with LPS (100 ng/ml) for the indicated time periods. **f, g** Immunoblotting of total and phosphorylated JNK, p38, and ERK in control, Lamtor5-expressing or Lamtor5-silenced RAW264.7 cells stimulated with LPS (100 ng/ml) for the indicated time periods. **h, i** Immunoblotting of total and phosphorylated TBK1 and IRF3 and **j, k** quantitative PCR to assess IFNβ production in control, Lamtor5-expressing, or Lamtor5-silenced RAW264.7 cells stimulated with LPS (100 ng/ml) for the indicated time periods. Representative images are shown, and the data from three independent experiments are expressed as the means ± SDs. *$P < 0.05$, **$P < 0.01$ by Student's *t*-test

docking was prevented when WT Lamtor5, but not mutant Lamtor5 (ΔLZ), was expressed (Fig. 6a). This finding prompted us to further examine whether the Lamtor5/TLR4 association affects mTORC1 localization at the lysosome. Intact TLR4, but not the truncated fragment (LRR) of TLR4, prevented the localization of mTORC1 at the lysosome (Fig. 6b). Accordingly, association-incompetent Lamtor5 or TLR4, unlike the intact Lamtor5 or TLR4 fragments (Fig. 4h), had no apparent effect on mTORC1 activation upon LPS stimulation (Fig. 6c).

Activated mTORC1 has been demonstrated to bind and phosphorylate TFEB, a master transcription factor responsible for the expression of autophagy-lysosome genes, which then causes the cytoplasmic retention of TFEB and hinders its nuclear translocation to trigger gene transcription.[36,48] Given that

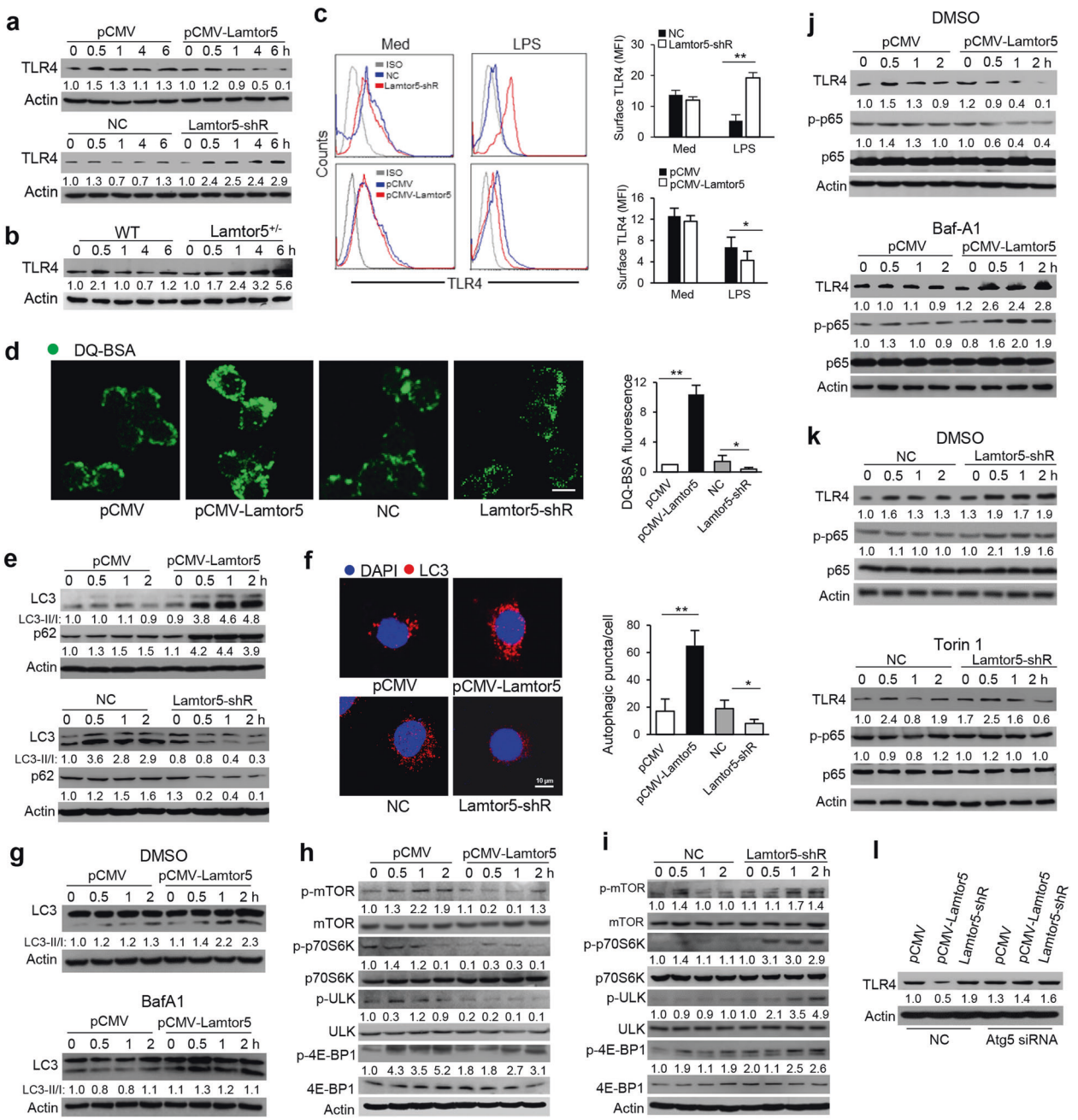

Fig. 4 Lamtor5 downregulates TLR4 levels by promoting autophagy. Immunoblotting for TLR4 in control, Lamtor5-expressing, and Lamtor5-silenced RAW264.7 cells (**a**) and Lamtor5$^{+/-}$ and WT macrophages (**b**) stimulated with LPS (100 ng/ml) for the indicated time periods. **c** FACS to assess surface TLR4 levels in control, Lamtor5-expressing, and Lamtor5-silenced RAW264.7 cells 2 h after LPS stimulation. Representative histograms and mean fluorescence intensities (MFIs) are shown. **d** Representative immunofluorescence images (left) and fluorescence quantification (right) of DQ-BSA activity in control, Lamtor5-expressing, and Lamtor5-silenced RAW264.7 cells. **e** Immunoblotting for LC3 and p62 in control, Lamtor5-expressing and Lamtor5-silenced RAW264.7 cells stimulated with LPS for the indicated time periods. **f** Representative confocal images showing LC3 puncta in control, Lamtor5-expressing and Lamtor5-silenced RAW264.7 cells stimulated with LPS for 2 h. Quantification of LC3 puncta per cell is also shown ($n = 100$ cells). **g** Immunoblotting for LC3 in control and Lamtor5-expressing RAW264.7 cells pretreated with DMSO or Baf-A1 and subjected to LPS stimulation for the indicated time periods. **h, i** Immunoblotting for the indicated proteins in control, Lamtor5-expressing, and Lamtor5-silenced RAW264.7 cells stimulated with LPS for the indicated time periods. **j** Immunoblotting for TLR4 and total and phosphorylated p65 in control and Lamtor5-expressing RAW264.7 cells pretreated with DMSO or Baf1 and then stimulated with LPS for the indicated time periods. **k** Immunoblotting for TLR4 and total and phosphorylated p65 in control and Lamtor5-silenced RAW264.7 cells pretreated with DMSO or torin 1 and then stimulated with LPS for the indicated time periods. **l** Immunoblotting for TLR4 in control, Lamtor5-expressing, and Lamtor5-silenced RAW264.7 cells transfected with nonspecific control (NC) or Atg5-specific siRNA, followed by LPS stimulation for 2 h. Representative images are shown, and data from three independent experiments are expressed as the means ± SDs. *$P < 0.05$, **$P < 0.01$ by Student's *t*-test

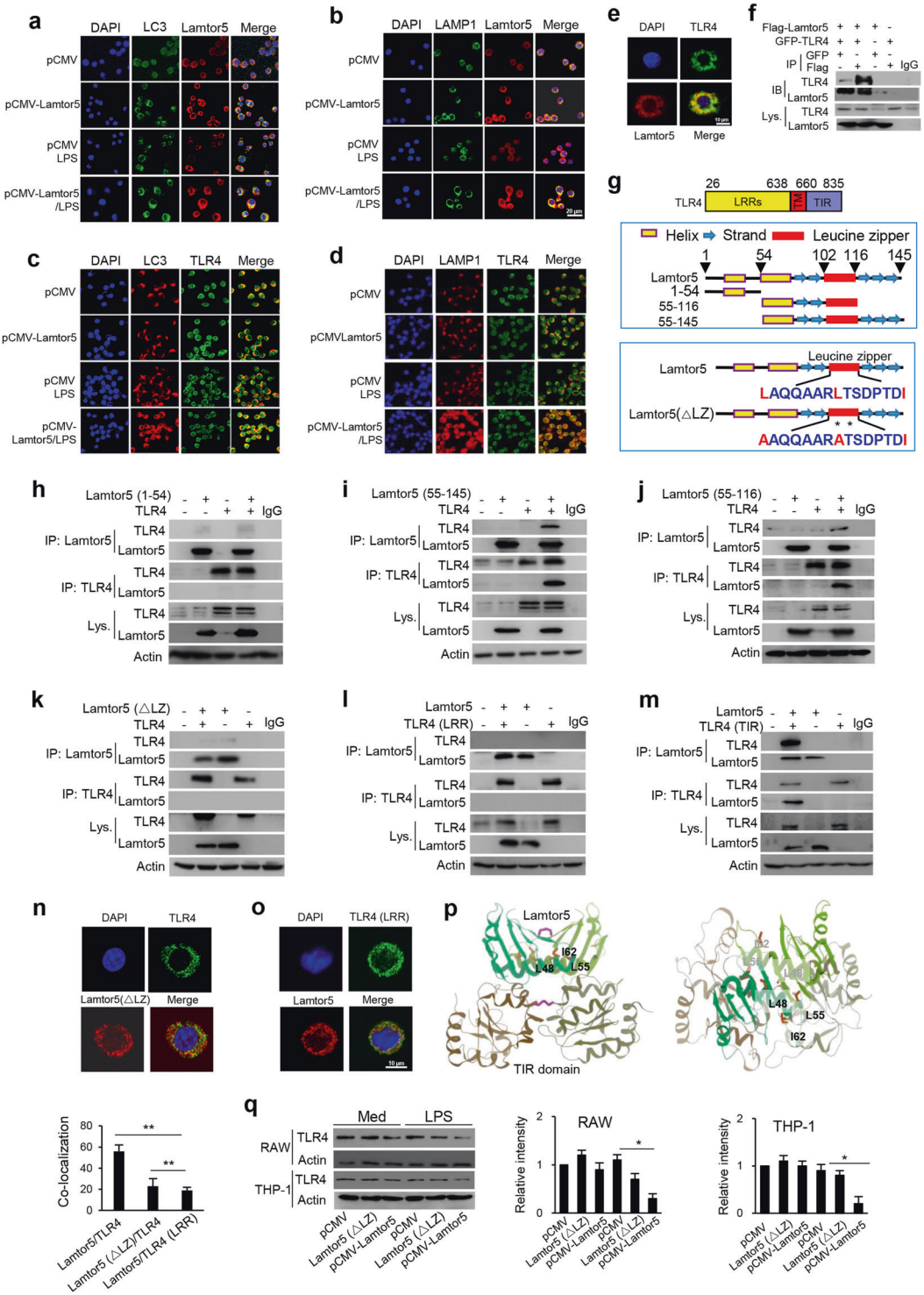

Fig. 5 Lamtor5 interacts with TLR4 and promotes its tethering at autolysosomes upon LPS stimulation. **a, b** Colocalization of Lamtor5 with LC3 or LAMP1 and **c, d** colocalization of TLR4 with LC3 or LAMP1 in control and Lamtor5-expressing RAW264.7 cells stimulated with LPS for 1 h. **e** Colocalization of TLR4 with Lamtor5 in RAW264.7 cells stimulated by LPS for 1 h. **f** Coimmunoprecipitation of Lamtor5 and TLR4 in 293T cells transfected with control, GFP-TLR4- and/or Flag-Lamtor5-expressing plasmids. IgG was used as a control. **g** Schematic illustration of the TLR4 structure and truncated TLR4 fragments (upper), the Lamtor5 structure and truncated Lamtor5 fragments (middle), and the LZ-mutant fragment (lower). **h–k** Coimmunoprecipitation of Lamtor5 and TLR4 in 293T cells transfected with plasmids harboring intact Lamtor5- or truncated/mutant Lamtor5-expressing plasmids with or without TLR4-expressing plasmids; **l, m** Coimmunoprecipitation of Lamtor5 and TLR4 in 293T cells transfected with plasmids encoding truncated TLR4 constructs and/or Lamtor5. **n, o** Colocalization of TLR4 with Lamtor5 in 293T cells transfected with intact Lamtor5- or mutant Lamtor5-expressing plasmid with or without TLR4-expressing plasmid. **p** Stereoview of the interaction between TLR4 (TIR) and Lamtor5 fragments using the I-TASSER server. Both TLR4 (TIR) and the Lamtor5 fragments are modeled as dimers, and the leucine zipper (LZ) structure at the interactive interface is shown. **q** Immunoblotting for TLR4 in RAW264.7 or THP-1 cells transfected with Lamtor5- or Lamtor5 (ΔLZ)-expressing plasmids. Quantified relative band intensities are also shown. Representative images are shown, and the data from three independent experiments are expressed as the means ± SDs. $^{*}P < 0.05$, $^{**}P < 0.01$ by Student's *t*-test

mTORC1 activation was suppressed upon Lamtor5 expression, the activity of its substrate, TFEB, is expected to be affected upon Lamtor5 expression. Indeed, the phosphorylation of TFEB was decreased upon Lamtor5 overexpression but enhanced by Lamtor5 knockdown following LPS stimulation (Fig. 6d). The nuclear translocation of TFEB was thus boosted upon Lamtor5 overexpression (Fig. 6e). Consequently, the expression of autophagy-lysosome genes was upregulated in Lamtor5-expressing macrophages but reduced in Lamtor5-silenced cells in response to LPS stimulation (Fig. 6f). TEM consistently demonstrated increased amounts of lysosome upon Lamtor5 expression (Fig. 6g). Moreover, our data indicated that Lamtor5 overexpression increased, while Lamtor5 knockdown hindered, lysosomal maturation, as detected with LysoSensor Green, a pH-sensing dye (Fig. 6h). To establish functional relevance, we showed that knockdown of TFEB largely abolished the Lamtor5-mediated reduction in TLR4 levels (Fig. 6i and Supplementary Fig. S6a). This result appeared to be related to abrogation of the Lamtor5-induced increase in LC3 fluorescence (Fig. 6j). Thus, the TFEB-driven autolysosomal pathway appears to be essential for Lamtor5-mediated regulation of TLR4 stability. We further tested this assumption by interfering with the autophagic pathway. Treatment with Rab7 siRNA or the autophagic inhibitor vinblastin[49] remarkably abrogated the suppressive effect of Lamtor5 on TLR4 levels (Supplementary Fig. S6b, c). In addition, the application of CQ, a putative neutralizer of lysosomal pH, or leupeptin, a lysosomal protease inhibitor, restored TLR4 levels in Lamtor5-expressing macrophages (Supplementary Fig. S6d, e). Collectively, our data indicated that Lamtor5, through recruiting and binding TLR4 at the autolysosome, dislodges, and inactivates mTOR and hence facilitates TFEB-driven autolysosomal processes.

Amino acid starvation reduces endotoxic shock via a Lamtor5-dependent mechanism

As Lamtor5 plays an essential role in the amino acid-sensing pathway[29] and nutrient status was shown to regulate the level of Lamtor5 in macrophages (Fig. 1j, k), we wondered whether Lamtor5 plays a role in coordinating immune and metabolic signaling. Intriguingly, deprivation of the EAA leucine significantly repressed the production of IL-6, TNF-α, and IL-1β in LPS-stimulated macrophages, which was at least partially abrogated upon the knockdown of Lamtor5 (Fig. 7a). In addition, leucine insufficiency had an anti-inflammatory effect on macrophages from WT control but not Lamtor5$^{+/-}$ mice (Fig. 7b). In addition, TLR4 levels were reduced upon leucine deprivation in control but not Lamtor5-silenced macrophages (Fig. 7c), implying that TLR4 is regulated by leucine deprivation in a Lamtor5-dependent manner. To further test this hypothesis in an in vivo system, we exploited a murine model of lung inflammation and injury induced by endotoxin challenge. Lung inflammation and injury, as exhibited by proinflammatory cell infiltration, proinflammatory cytokine production, protein leakage and lung MPO activity, were alleviated in mice fed a leucine-free diet (leu-), but this effect was largely abrogated in Lamtor5 haploinsufficient mice (Fig. 7d–h). Moreover, mice fed a leucine-free diet exhibited a survival advantage over littermates fed a normal diet when challenged with a lethal dose of endotoxin. However, this elevated survival rate upon leucine deprivation appeared to be abrogated in Lamtor5$^{+/-}$ mice (Fig. 7i), implying that the anti-inflammatory effect of leucine deletion is at least partially mediated through Lamtor5 functioning.

DISCUSSION

In the present study, we elucidate an unexpected key role for Lamtor5, a newly identified amino acid-sensing protein, in modulating TLR4 signaling and inflammatory responses. Importantly, Lamtor5 impacted TLR4 intracellular trafficking, promoted its autophagic degradation, and controlled inflammatory signaling. We demonstrate that the physical association of Lamtor5 with TLR4 facilitated their colocalization at LC3^{+}LAMP^{+} autolysosomes and thereby hindered mTORC1 lysosomal tethering and activation upon LPS stimulation, which in turn derepressed TFEB to activate the autolysosomal program and promote TLR4 degradation. Accordingly, Lamtor5 deficiency caused uncontrolled TLR4 signaling and increased susceptibility to endotoxic shock and lung injury; we have thus elucidated a hitherto unknown role of Lamtor5 in TLR biology and identified a novel catabolic mechanism essential for immune homeostasis (Fig. 7j). Interestingly, Lamtor5 was induced by not only inflammatory insult but also by nutrient stress, specifically deprivation of the EAA leucine. Lamtor5, mostly likely through promoting TLR4 degradation, mediated the anti-inflammatory effect of leucine deprivation and contributed to the alleviation of inflammatory pathology in mice fed a leucine-free diet.[39] We thus propose a Lamtor5-centered regulatory paradigm that integrates inflammatory and metabolic cues to shape immune and inflammatory responses; this model may have implications for TLR4-associated metabolic inflammation.[50,51]

An increasing amount of data indicate that cellular degradative system is a dynamic and complex vacuolar network that also involves the autophagosome, a canonical catabolic structure responsible for the clearance of intracellular molecules or organelles. TLR engagement on macrophages has been demonstrated to trigger the generation of LC3^{+} autophagosomes or promote LC3 recruitment to endosomes or phagosomes, resulting in activation of the autolysosomal pathway in an ATG5/7-dependent manner.[21,52] The autolysosomal machinery has been implicated in TLR-mediated responses, but its exact role and the involved mechanism remain largely unknown.[53] Our present study demonstrates that the cellular catalytic process controlled by Lamtor5 is essential for the autophagic degradation of TLR4 and homeostatic control of inflammation.

Lamtor5 regulates TLR4 on at least two levels: the association and recruitment of TLR4 to degradation vacuoles and regulation of the autolysosomal pathway. Lamtor5 specifically associates with TLR4 through the TIR/LZ interaction, as disruption of the Lamtor5 LZ domain or deletion of the TLR4 TIR fragment almost completely abrogated their association and subsequent TLR4 degradation. Computer-aided structural predictive analysis further substantiated the feasibility and reliability of the TIR/LZ interaction between these two molecules. We have thus identified Lamtor5 as an unconventional adaptor without a TIR domain capable of interacting with TLR4 in a site-specific manner[54] that is essential for TLR4 recruitment to autolysosomes. Indeed, Lamtor5 has been reported to act as a scaffold in its interactions with Rag GTPases, c-FOS, c-Myc, Survivin, and p53.[26–28] Intriguingly, the LZ domain is required for the association of Lamtor5 c-FOS and c-Myc but not Survivin, implying that Lamtor5 recognizes and interacts with different substrates with different site preferences. In addition, environmental conditions, particularly pH, were shown to affect the conformation of Lamtor5 and hence its affinity to binding partners. A low pH (5.0–5.6) was favorable for a folded and hence more stable and accessible Lamtor5 structure, whereas Lamtor5 was more unstructured and unstable and bound its partners with a lower affinity in basic conditions (pH 8.3).[46] This finding seems compatible with our currently proposed model that Lamtor5 promotes the biogenesis and maturation of lysosomes upon LPS stimulation, generating acidic, and amenable conditions for its association with TLR4, whereas low levels of Lamtor5 in resting macrophages yield immature and nonacidic lysosomes, preventing the binding of TLR4 to Lamtor5. Thus, Lamtor5 functioning serves as a pH-sensitive and lysosome-dependent feedback mechanism to control ongoing inflammation.

Aside from its role as an anchor for internalized TLR4, Lamtor5 also plays a critical role in promoting the autolysosomal pathway through regulating the mTOR/TFEB axis. TLR4 signaling has been

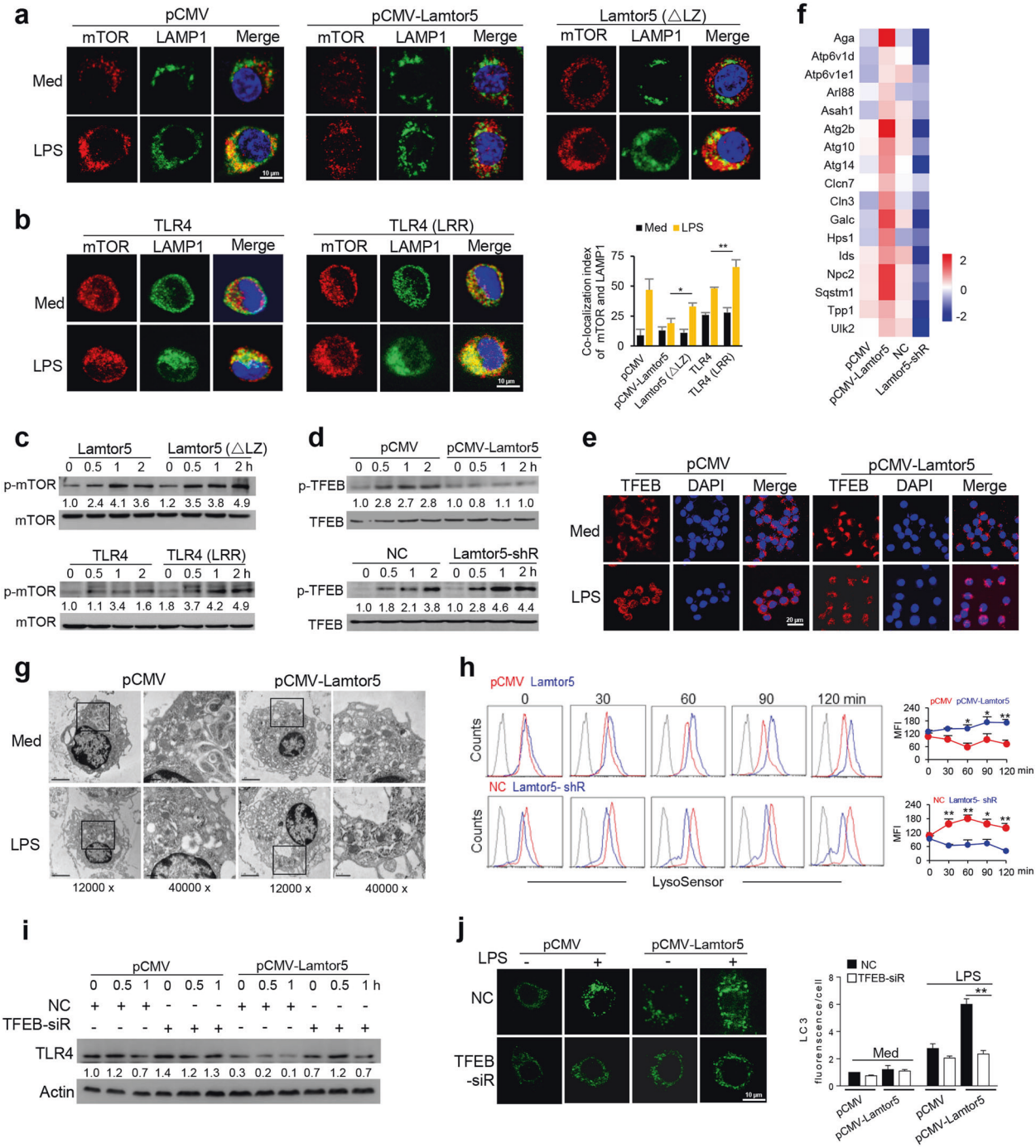

Fig. 6 Lamtor5 enhances the autolysosomal gene program via regulating the mTOR/TFEB axis. **a** Colocalization of mTOR and LAMP1 in control, Lamtor5- or mutant Lamtor5 (ΔLZ)-expressing RAW264.7 cells treated with or without LPS for 1 h. **b** Colocalization of mTOR and LAMP1 in RAW264.7 cells transfected with intact TLR4- or truncated TLR4 (LRR)-expressing plasmids with or without LPS stimulation for 1 h. **c** Immunoblotting for total and phosphorylated mTOR in RAW264.7 cells transfected with Lamtor5- or Lamtor5 (ΔLZ)-expressing plasmids (upper) or TLR4-/- macrophages transfected with intact TLR4 or truncated TLR4 (LRR) (lower) upon stimulation with LPS for the indicated time periods. **d** Immunoblotting for phosphorylated and total TFEB in control, Lamtor5-expressing, and Lamtor5-silenced RAW264.7 cells stimulated with LPS for the indicated time periods. **e** Immunostaining for TFEB in control and Lamtor5-expressing RAW264.7 cells stimulated with LPS for 1 h. **f** Heat map showing the levels of autophagy-lysosome genes in control, Lamtor5-expressing or Lamtor5-silenced RAW264.7 cells stimulated with LPS for 3 h. **g** Transmission electron microscopy (TEM) of RAW264.7 cells transfected with control and Lamtor5-expressing plasmids with or without LPS stimulation. Black box, lysosomes. **h** Control, Lamtor5-expressing or Lamtor5-silenced RAW264.7 cells were stained with LysoSensor Green and analyzed by FACS. Representative histograms (lower) and relative fluorescence quantification (upper) are shown. **i** Immunoblotting for TLR4 in control and Lamtor5-expressing RAW264.7 cells transfected with nonspecific control (NC) or TFEB-targeted siRNA followed by LPS stimulation for the indicated time periods. **j** Confocal microscopy showing LC3 puncta in control and Lamtor5-expressing RAW264.7 cells transfected with nonspecific control (NC) or TFEB-targeted siRNA followed by LPS stimulation for 1 h. Representative images (left) and the quantification of LC3 puncta (100 cells) are shown (right). Data are from three independent experiments and expressed as the means ± SDs. $^{*}P < 0.05$, $^{**}P < 0.01$ by Student's *t*-test

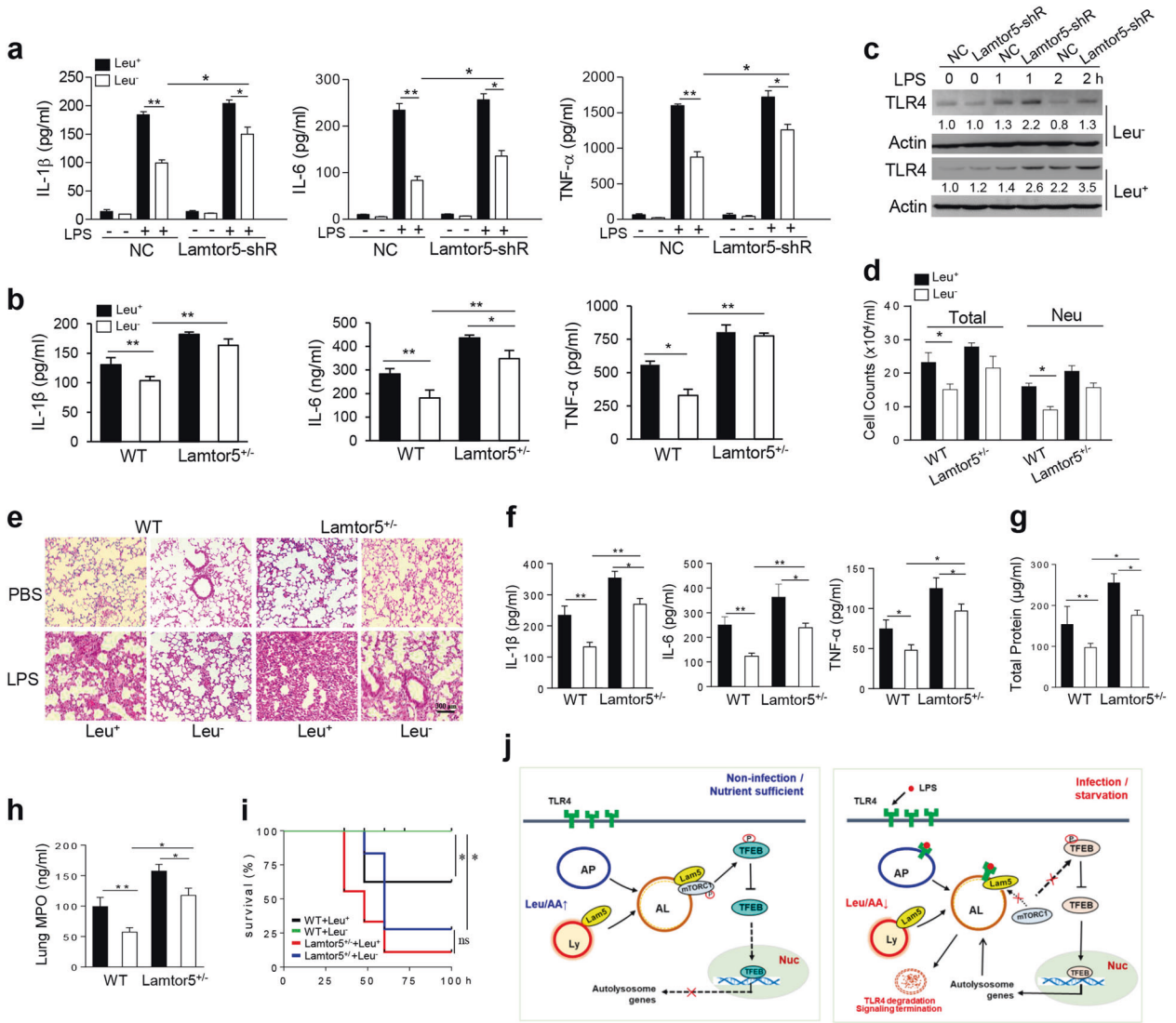

Fig. 7 Lamtor5 partially mediates the anti-inflammatory effect of leucine deprivation. **a** Production of proinflammatory cytokines by control and Lamtor5-silenced RAW264.7 cells or **b** macrophages from WT and Lamtor5$^{+/-}$ mice. Cells were cultured in complete (Leu^{+}) and leucine-depleted (Leu^{-}) media and stimulated with LPS for 12 h. Levels of the indicated cytokines in cellular supernatants were analyzed by ELISA. **c** TLR4 levels in control and Lamtor5-silenced RAW264.7 cells cultured in complete (Leu^{+}) and leucine-depleted (Leu^{-}) media stimulated with LPS for the indicated time periods. Relative intensities were quantified and are shown below each corresponding band. **d**–**h** WT and Lamtor5$^{+/-}$ mice ($n = 5$) were fed a normal (Leu^{+}) or leucine-deficient (Leu^{-}) diet for 1 week and then received LPS treatment (1 mg/kg, i.t.) for 12 h. Cell counts (**d**), H&E staining of lung sections (**e**), BALF cytokine levels (**f**) and protein leakage (**g**), lung MPO activity (**h**). All the data are from three independent experiments and expressed as the means ± SDs. *$P < 0.05$, **$P < 0.01$ by Student's *t*-test. **i** WT and Lamtor5$^{+/-}$ mice ($n = 10$–12) were fed a normal (Leu^{+}) or leucine-depleted diet (Leu^{-}) and challenged with LPS (12 mg/kg, i.p.), following which the survival rate was analyzed by the Kaplan–Meier method. **j** A proposed working model indicating that Lamtor5 plays dual roles in both associating with/recruiting TLR4 and regulating the TFEB-driven autolysosomal pathway, thereby contributing to the autophagic degradation of TLR4 and inflammation termination. AA amino acid, AP autophagosome, AL autolysosome, Ly lysosome, Lam5 Lamtor5, Leu leucine, Nuc nucleus

demonstrated to trigger mTOR, but the functional relevance of mTOR to TLR4 signaling remains controversial.[55,56] Our current study reveals that mTORC1, which is controlled by Lamtor5, plays a unique role in promoting TLR4 signaling through counteracting autophagy. Although the exact mechanism by which Lamtor5 modulates mTORC1 is not understood at this stage, our initial data indicate that the association and colocalization of Lamtor5 and TLR4 significantly hinders the lysosomal docking of mTORC1 and thus prevents its activation. mTORC1 may be inaccessible due to altered lysosomal architecture upon Lamtor5/TLR4 ligation or the formation of a compact TLR4/Lamtor5 structure that blocks mTORC1 tethering.[57] This hypothesis is likely supported by the recent finding that the Lamtor5-containing Ragulator complex forms a tightly bound supercomplex with v-ATPase and Rag GTPases that inhibits lysosome docking and activation of mTORC1 upon amino acid insufficiency. Alternatively, the suppression of mTORC1 by Lamtor5 might be attributed to its promotion of the activation of AMP-activated protein kinase (AMPK), a putative mTORC1 inhibitor,[58] in response to LPS stimulation (Supplementary Fig. S7).

Intriguingly, the Lamtor5-mediated inhibition of mTORC1 is seemingly at odds with the requirement of Lamtor5 for mTORC1 activation upon amino acid stimulation. This discrepancy might be attributed to the context-dependent function of Lamtor5. In fact, Lamtor5 is not the sole Ragulator member that exerts an inhibitory effect on mTORC1 activity. Lamtor2, another Ragulator molecule,

was shown to repress mTORC1 activity in dendritic cells (DCs), leading to rapid degradation of the Fms-like tyrosine kinase 3 receptor and limiting DC activity.[59] Lamtor1 can also promote the autolysosomal pathway, a process presumably repressed by mTORC1, and plays a central role in epidermal development.[60] These results reveal the intimate relationship between mTOR and Lamtor family members, which appears to be essential for immune homeostasis.

Despite an increasing appreciation for the importance of autolysosomes in immune and inflammatory responses, how this degradative machinery reacts to external signals and contributes to optimized immune and inflammatory responses remains elusive. We herein have identified TFEB, a master transcriptional factor for autolysosome genes, as an effector molecule of Lamtor5 that translates inflammatory information into the regulatory system for TLR4 signaling. In response to nutrients and growth factors, TFEB is phosphorylated by mTORC1 and subsequently bound by 14–3–3 proteins for cytosolic sequestration.[36,61] Nutrient starvation, however, leads to mTORC1 inaction and the consequent depression of TFEB, allowing its entry into the nucleus to activate autolysosomal genes. Our current study expands upon the functions of TFEB by demonstrating its importance in mediating the cellular response to pathogenic insults such as bacterial endotoxin. Upon LPS stimulation, TFEB is released from mTORC1-mediated inhibition, which is suppressed by Lamtor5, promoting autolysosome biogenesis and expediting TLR4 processing. The mTOR/TFEB axis appears to function as a balanced system that guarantees the TLR4-driven response to be comprehensive but not excessive.

Another interesting finding of our present study is that Lamtor5 plays a role in coordinating inflammatory and metabolic cues to shape the optimized host response. Lamtor5, most likely through accelerating the autophagic degradation of TLR4, mediated the anti-inflammatory effect of leucine deprivation and protected against endotoxic sepsis in mice fed a leucine-free diet; these results may confer mechanistic insight into so-called "starving inflammation".[62] Recently, Zhao et al. identified transmembrane BAX inhibitor motif-containing 1 (TMBIM1) as a negative regulator of TLR4 signaling that also plays a role in suppressing hepatic steatosis and inflammation.[63] Similar to our findings, the multivesicular body-lysosomal pathway was identified as a key mechanism responsible for TMBIM1-mediated TLR4 degradation and immune and metabolic balance. Given that the TLR4 pathway is frequently aberrantly activated during metabolic diseases,[64,65] further studies on the potential role of Lamtor5 in TLR4-associated metabolic inflammation may be warranted.

In summary, we have uncovered hitherto unknown roles of Lamtor5 in regulating TLR4 fate and maintaining immune homeostasis. We also show that Lamtor5 is essential in coordinating nutrient and inflammatory cues to shape the optimized immune response, which may shed new light on immunometabolic disorders.

ACKNOWLEDGEMENTS

This work was supported by National Natural Scientific Funds (81770014 and 81470210), the National Key Research and Development Program Project (2018YFC1705900), the Natural Science Foundation of Jiangsu Province Fund (BK20180824), financial support for the Jiangsu Key Laboratory for Pharmacology and Safety Evaluation of Chinese Materia Medica, and the Priority Academic Program Development of Jiangsu Higher Education Institutions.

AUTHOR CONTRIBUTIONS

L.S. designed the project. W.Z., N.Z., L.H., X.L., Y.H., M.P., H.Z. and Y.K. performed experiments and analyzed data. Y.L., D.X. and Q.W. contributed to the experimental material and provided insightful suggestions. L.S. and W.Z. wrote the manuscript.

ADDITIONAL INFORMATION

The online version of this article (https://doi.org/10.1038/s41423-019-0281-6) contains supplementary material.

Competing interests: The authors declare no competing interests.

REFERENCES

1. Kawai, T. & Akira, S. The role of pattern-recognition receptors in innate immunity: update on toll-like receptors. *Nat. Immunol.* **11**, 373–384 (2010).
2. Liu, J. & Cao, X. Cellular and molecular regulation of innate inflammatory responses. *Cell. Mol. Immunol.* **13**, 711–721 (2016).
3. Medzhitov, R. Origin and physiological roles of inflammation. *Nature* **454**, 428–435 (2008).
4. Brubaker, S. W., Bonham, K. S., Zanoni, I. & Kagan, J. C. Innate immune pattern recognition: a cell biological perspective. *Annu. Rev. Immunol.* **33**, 257–290 (2015).
5. Gay, N. J., Symmons, M. F., Gangloff, M. & Bryant, C. E. Assembly and localization of Toll-like receptor signalling complexes. *Nat. Rev. Immunol.* **14**, 546–558 (2014).
6. Kagan, J. C. et al. TRAM couples endocytosis of toll-like receptor 4 to the induction of interferon-beta. *Nat. Immunol.* **9**, 361–368 (2008).
7. O'Neill, L. A., Golenbock, D. & Bowie, A. G. The history of toll-like receptors—redefining innate immunity. *Nat. Rev. Immunol.* **13**, 453–460 (2013).
8. Wang, Y. et al. Lysosome-associated small Rab GTPase Rab7b negatively regulates TLR4 signaling in macrophages by promoting lysosomal degradation of TLR4. *Blood* **110**, 962–971 (2007).
9. Kagan, J. C. Recycling endosomes and TLR signaling-the Rab11 GTPase leads the way. *Immunity* **33**, 578–580 (2010).
10. Wang, D. et al. Ras-related protein Rab10 facilitates TLR4 signaling by promoting replenishment of TLR4 onto the plasma membrane. *Proc. Natl Acad. Sci. USA* **107**, 13806–13811 (2010).
11. Liaunardy-Jopeace, A., Bryant, C. E. & Gay, N. J. The COP II adaptor protein TMED7 is required to initiate and mediate the delivery of TLR4 to the plasma membrane. *Sci. Signal.* **7**, ra70 (2014).
12. Bonham, K. S. et al. A promiscuous lipid-binding protein diversifies the subcellular sites of Toll-like receptor signal transduction. *Cell* **156**, 705–716 (2014).
13. Jakka, P. et al. Cytoplasmic linker protein CLIP170 negatively regulates TLR4 signaling by targeting the TLR adaptor protein TIRAP. *J. Immunol.* **200**, 704–714 (2018).
14. Kaur, J. & Debnath, J. Autophagy at the crossroads of catabolism and anabolism. *Nat. Rev. Mol. cell Biol.* **16**, 461–472 (2015).
15. Mizushima, N. & Komatsu, M. Autophagy: renovation of cells and tissues. *Cell* **147**, 728–741 (2011).
16. Jiang, P. & Mizushima, N. Autophagy and human diseases. *Cell Res.* **24**, 69–79 (2014).
17. Cadwell, K. Crosstalk between autophagy and inflammatory signalling pathways: balancing defence and homeostasis. *Nat. Rev. Immunol.* **16**, 661–675 (2016).
18. Saitoh, T. et al. Loss of the autophagy protein Atg16L1 enhances endotoxin-induced IL-1beta production. *Nature* **456**, 264–268 (2008).
19. Acharya, M. et al. Alphav Integrins combine with LC3 and atg5 to regulate toll-like receptor signalling in B cells. *Nat. Commun.* **7**, 10917 (2016).
20. Xu, Y. et al. Toll-like receptor 4 is a sensor for autophagy associated with innate immunity. *Immunity* **27**, 135–144 (2007).
21. Sanjuan, M. A. et al. Toll-like receptor signalling in macrophages links the autophagy pathway to phagocytosis. *Nature* **450**, 1253–1257 (2007).
22. Yang, Q. et al. TRIM32-TAX1BP1-dependent selective autophagic degradation of TRIF negatively regulates TLR3/4-mediated innate immune responses. *PLoS Pathog.* **13**, e1006600 (2017).
23. Fujita, K., Maeda, D., Xiao, Q. & Srinivasula, S. M. Nrf2-mediated induction of p62 controls toll-like receptor-4-driven aggresome-like induced structure formation and autophagic degradation. *Proc. Natl Acad. Sci. USA* **108**, 1427–1432 (2011).
24. Giegerich, A. K. et al. Autophagy-dependent PELI3 degradation inhibits proinflammatory IL1B expression. *Autophagy* **10**, 1937–1952 (2014).
25. Melegari, M., Scaglioni, P. P. & Wands, J. R. Cloning and characterization of a novel hepatitis B virus x binding protein that inhibits viral replication. *J. Virol.* **72**, 1737–1743 (1998).
26. Li, Y. et al. HBXIP and LSD1 scaffolded by lncRNA hotair mediate transcriptional activation by c-Myc. *Cancer Res.* **76**, 293–304 (2016).
27. Marusawa, H. et al. HBXIP functions as a cofactor of survivin in apoptosis suppression. *EMBO J.* **22**, 2729–2740 (2003).
28. Li, H. et al. The oncoprotein HBXIP modulates the feedback loop of MDM2/p53 to enhance the growth of breast cancer. *J. Biol. Chem.* **290**, 22649–22661 (2015).

29. Bar-Peled, L., Schweitzer, L. D., Zoncu, R. & Sabatini, D. M. Ragulator is a GEF for the rag GTPases that signal amino acid levels to mTORC1. *Cell* **150**, 1196–1208 (2012).
30. Sancak, Y. et al. Ragulator-rag complex targets mTORC1 to the lysosomal surface and is necessary for its activation by amino acids. *Cell* **141**, 290–303 (2010).
31. Zoncu, R. et al. mTORC1 senses lysosomal amino acids through an inside-out mechanism that requires the vacuolar H(+)-ATPase. *Science* **334**, 678–683 (2011).
32. Rebsamen, M. et al. SLC38A9 is a component of the lysosomal amino acid sensing machinery that controls mTORC1. *Nature* **519**, 477–481 (2015).
33. Marichal, T. et al. Guanine nucleotide exchange factor RABGEF1 regulates keratinocyte-intrinsic signaling to maintain skin homeostasis. *J. Clin. Investig.* **126**, 4497–4515 (2016).
34. Tang, S. et al. RasGRP3 limits toll-like receptor-triggered inflammatory response in macrophages by activating Rap1 small GTPase. *Nat. Commun.* **5**, 4657 (2014).
35. Yang, C. W. et al. Regulation of T cell receptor signaling by DENND1B in TH2 cells and allergic disease. *Cell* **164**, 141–155 (2016).
36. Settembre, C. et al. TFEB links autophagy to lysosomal biogenesis. *Science* **332**, 1429–1433 (2011).
37. Cong, L. et al. Multiplex genome engineering using CRISPR/Cas systems. *Science* **339**, 819–823 (2013).
38. Kang, Y. et al. MAPK kinase 3 potentiates Chlamydia HSP60-induced inflammatory response through distinct activation of NF-kappaB. *J. Immunol.* **191**, 386–394 (2013).
39. Ravindran, R. et al. The amino acid sensor GCN2 controls gut inflammation by inhibiting inflammasome activation. *Nature* **531**, 523–527 (2016).
40. Shi, B. et al. SNAPIN is critical for lysosomal acidification and autophagosome maturation in macrophages. *Autophagy* **13**, 285–301 (2017).
41. Liang, C. et al. Beclin1-binding UVRAG targets the class C Vps complex to coordinate autophagosome maturation and endocytic trafficking. *Nat. cell Biol.* **10**, 776–787 (2008).
42. Yang, J. & Zhang, Y. I-TASSER server: new development for protein structure and function predictions. *Nucleic acids Res.* **43**, W174–W181 (2015).
43. Xu, Y. et al. Structural basis for signal transduction by the Toll/interleukin-1 receptor domains. *Nature* **408**, 111–115 (2000).
44. Phillips, J. C. et al. Scalable molecular dynamics with NAMD. *J. Comput. Chem.* **26**, 1781–1802 (2005).
45. Tanner, D. E., Chan, K. Y., Phillips, J. C. & Schulten, K. Parallel generalized born implicit solvent calculations with NAMD. *J. Chem. Theory Comput.* **7**, 3635–3642 (2011).
46. Garcia-Saez, I., Lacroix, F. B., Blot, D., Gabel, F. & Skoufias, D. A. Structural characterization of HBXIP: the protein that interacts with the anti-apoptotic protein survivin and the oncogenic viral protein HBx. *J. Mol. Biol.* **405**, 331–340 (2011).
47. Park, B. S. et al. The structural basis of lipopolysaccharide recognition by the TLR4-MD-2 complex. *Nature* **458**, 1191–1195 (2009).
48. Settembre, C. et al. A lysosome-to-nucleus signalling mechanism senses and regulates the lysosome via mTOR and TFEB. *EMBO J.* **31**, 1095–1108 (2012).
49. Munafo, D. B. & Colombo, M. I. A novel assay to study autophagy: regulation of autophagosome vacuole size by amino acid deprivation. *J. cell Sci.* **114**, 3619–3629 (2001).
50. Konner, A. C. & Bruning, J. C. Toll-like receptors: linking inflammation to metabolism. *Trends Endocrinol. Metab.: TEM* **22**, 16–23 (2011).
51. O'Neill, L. A. & Pearce, E. J. Immunometabolism governs dendritic cell and macrophage function. *J. Exp. Med.* **213**, 15–23 (2016).
52. Delgado, M. A., Elmaoued, R. A., Davis, A. S., Kyei, G. & Deretic, V. Toll-like receptors control autophagy. *EMBO J.* **27**, 1110–1121 (2008).
53. Netea-Maier, R. T., Plantinga, T. S., van de Veerdonk, F. L., Smit, J. W. & Netea, M. G. Modulation of inflammation by autophagy: Consequences for human disease. *Autophagy* **12**, 245–260 (2016).
54. Luo, L. et al. SCIMP is a transmembrane non-TIR TLR adaptor that promotes proinflammatory cytokine production from macrophages. *Nat. Commun.* **8**, 14133 (2017).
55. Weichhart, T. et al. The TSC-mTOR signaling pathway regulates the innate inflammatory response. *Immunity* **29**, 565–577 (2008).
56. Luo, L. et al. Rab8a interacts directly with PI3Kgamma to modulate TLR4-driven PI3K and mTOR signalling. *Nat. Commun.* **5**, 4407 (2014).
57. Schweitzer, L. D., Comb, W. C., Bar-Peled, L. & Sabatini, D. M. Disruption of the rag-ragulator complex by c17orf59 inhibits mTORC1. *Cell Rep.* **12**, 1445–1455 (2015).
58. Gwinn, D. M. et al. AMPK phosphorylation of raptor mediates a metabolic checkpoint. *Mol. cell* **30**, 214–226 (2008).
59. Scheffler, J. M. et al. LAMTOR2 regulates dendritic cell homeostasis through FLT3-dependent mTOR signalling. *Nat. Commun.* **5**, 5138 (2014).
60. Soma-Nagae, T. et al. The lysosomal signaling anchor p18/LAMTOR1 controls epidermal development by regulating lysosome-mediated catabolic processes. *J. cell Sci.* **126**, 3575–3584 (2013).
61. Martina, J. A., Chen, Y., Gucek, M. & Puertollano, R. MTORC1 functions as a transcriptional regulator of autophagy by preventing nuclear transport of TFEB. *Autophagy* **8**, 903–914 (2012).
62. Buck, M. D., Sowell, R. T., Kaech, S. M. & Pearce, E. L. Metabolic Instruction of Immunity. *Cell* **169**, 570–586 (2017).
63. Zhao, G. N. et al. Tmbim1 is a multivesicular body regulator that protects against non-alcoholic fatty liver disease in mice and monkeys by targeting the lysosomal degradation of Tlr4. *Nat. Med.* **23**, 742–752 (2017).
64. Uchimura, K. et al. The serine protease prostasin regulates hepatic insulin sensitivity by modulating TLR4 signalling. *Nat. Commun.* **5**, 3428 (2014).
65. Pal, D. et al. Fetuin-A acts as an endogenous ligand of TLR4 to promote lipid-induced insulin resistance. *Nat. Med.* **18**, 1279–1285 (2012).